

図3 CVD 治療が有効であった1例 (60歳男性, 左腎門部パラガングリオーマ)

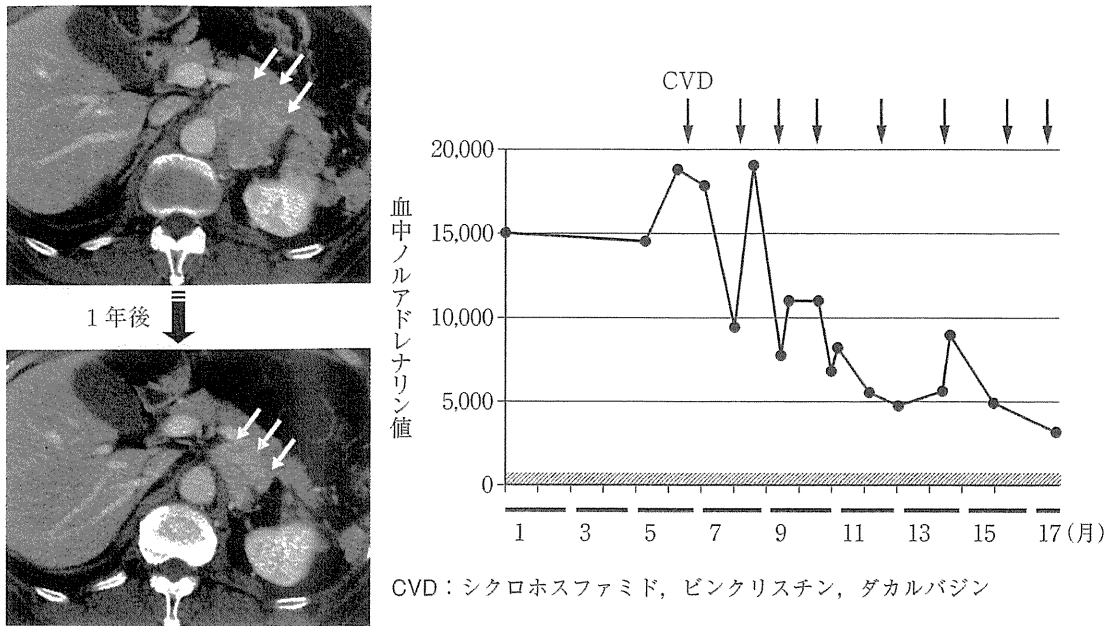


表3 悪性褐色細胞腫・パラガングリオーマにおけるスニチニブの治療効果に関する報告

| No. | 診断               | 用量   | n | 効果             |    | 年・文献 No. | 備考   |
|-----|------------------|--|---|----------------|----|----------|--|
|     |                  |  |   | CR             | PR |          |  |
| 1   | 転移性<br>パラガングリオーマ | 50mg daily<br>4wk on,<br>2wk off           | 3 | 1<br>(near CR) | 2  | 2009年・6) | 2~3サイクル施行後に治療効果出現.                             |
| 2   | 悪性褐色細胞腫<br>(VHL) | Single dose<br>for 28-d of<br>a 42-d cycle | 1 | -              | 1  | 2009年・7) | 6ヵ月後には症状改善し, 内分泌学的にも画像上も改善.                    |
| 3   | 悪性褐色細胞腫          | 37.5mg daily                               | 1 | -              | 1  | 2009年・8) | 7週後に胸水貯留, 呼吸困難のため中止. 休薬後, 胸水改善したため 25mg/d で再開. |

CR: 完全寛解, PR: 部分寛解

2. 主な副作用

骨髄抑制, 高血圧, 心不全, 感染症が主な副作用である. 骨髄抑制は白血球の減少, 貧血, 特に血小板減少症の頻度が高い. 消化器症状として食欲低下, 嘔気, 下痢のほか, まれに消化管穿孔が報告されている. 粘膜・皮膚症状として口内炎, 皮膚変色, 発疹, 脱毛などを認める.

その他, 不整脈, 心機能低下, 高血圧も報告されている.

まとめ

悪性褐色細胞腫は確立された薬物治療がなく難治性疾患である. CVD 治療は根治的療法ではなく, 長期予後への影響も不明である. しか

しながら、低～中等度の副作用で一部の症例に有効であること、本邦では<sup>131</sup>I-MIBG治療の施行が限定的であることから、現時点ではCVD治療が抗腫瘍治療の第1選択となっている。悪性褐色細胞腫では、高カテコールアミン血症がADL低下や死因に関与することから、限定的な期間でもCVD治療によりカテコールアミンのコントロールが可能であれば、QOLと予後の向上の点で考慮すべき治療と言える。また分子標的薬の有効性が報告されつつあるが、悪性褐色細胞腫には適応外で、今後より多数例での臨床試験の実施が期待される。

#### 文 献

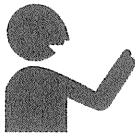
- 1) Mishra A K, et al: Catecholamine cardiomyopathy in bilateral malignant pheochromocytoma: successful reversal after surgery. *Int J Cardiol* 76 (1): 89-90, 2000.
- 2) Averbuch S D, et al: Malignant pheochromocytoma: effective treatment with a combination of cyclophosphamide, vincristine, and dacarbazine. *Ann Intern Med* 109 (4): 267-273, 1988.
- 3) Wu L T, et al: Hypertensive crises induced by treatment of malignant pheochromocytoma with a combination of cyclophosphamide, vincristine, and dacarbazine. *Med Pediatr Oncol* 22 (6): 389-392, 1994.
- 4) Noshiro T, et al: Two cases of malignant pheochromocytoma treated with cyclophosphamide, vincristine and dacarbazine in a combined chemotherapy. *Endocr J* 43: 279-284, 1996.
- 5) van der Harst E, et al: Proliferative index in phaeochromocytomas: does it predict the occurrence of metastases? *J Pathol* 191: 175-180, 2000.
- 6) Joshua A M, et al: Rationale and evidence for sunitinib in the treatment of malignant paraganglioma/pheochromocytoma. *J Clin Endocrinol Metab* 94 (1): 5-9, 2009.
- 7) Jimenez C, et al: Use of the tyrosine kinase inhibitor sunitinib in a patient with von Hippel-Lindau disease: targeting angiogenic factors in pheochromocytoma and other von Hippel-Lindau disease-related tumors. *J Clin Endocrinol Metab* 94 (2): 386-391, 2009.
- 8) Park K S, et al: Sunitinib, a novel therapy for anthracycline- and cisplatin-refractory malignant pheochromocytoma. *Jpn J Clin Oncol* 39 (5): 327-331, 2009.
- 9) Study of Sunitinib in Patients with Recurrent Paraganglioma/Pheochromocytoma (SNIPP). University Health Network, Toronto.

#### Medical Treatments of Malignant Pheochromocytoma

Mitsuhide Naruse<sup>1</sup>, Mika Tsuiki<sup>2</sup>, Kanako Nakao<sup>1</sup>,  
Kazutaka Nanba<sup>1</sup>, Tamiko Tamanaha<sup>1</sup>, Akiyo Tanabe<sup>1,2</sup>

<sup>1</sup> Department of Endocrinology, Metabolism, and Hypertension,  
National Hospital Organization Kyoto Medical Center

<sup>2</sup> Department of Medicine, Tokyo Women's Medical University



## 話題

# 褐色細胞腫診療と研究の現状と課題\*

成瀬 光栄\*\* 立木 美香\*\*\* 田辺 晶代\*\*\*

**Key Words** : pheochromocytoma, succinyl dehydrogenase, metastasis, open-pheonetwork, malignant pheochromocytoma

### はじめに

褐色細胞腫は治癒可能な内分泌性高血圧症の代表的疾患で、実際、その80~90%は適切な診断と治療により完治する。しかしながら、同じく内分泌性高血圧症の代表とされる原発性アルドステロン症とはまったく異なり、その約10%が悪性腫瘍である点が特徴である。病理学的には‘悪性’との表現よりも‘低分化’との表現が用いられるが、臨床医にとって診療上の実感としてよりわかりやすいことから、一般に‘悪性褐色細胞腫’の表現を用いる。本疾患は早期診断が困難かつ診断されても治療が困難な難治性疾患で、

医学データベースにおける本疾患の論文数(図1)は飛躍的に増加している。医学的にも医療面からも今後解決すべきさまざまな課題があることから、日本内分泌学会の臨床重要課題に指定され、厚生労働省難治性疾患の調査対象ともなっている。本稿では、本疾患の診断と治療に関する最近の話題につき解説する<sup>1)~9)</sup>。

### 臨床的課題(表1)

臨床的に次の5点が課題といえる。

#### 1. 第一の課題

悪性例が多いことである。厚生省副腎ホルモン産生異常症調査研究班(名和田 新班長)の全

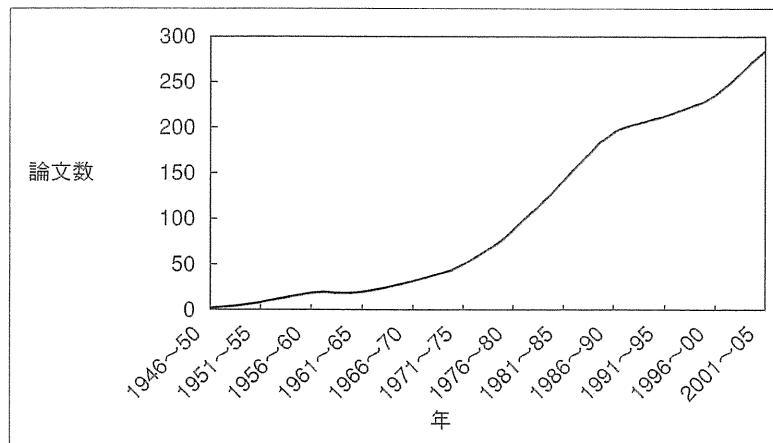


図1 悪性褐色細胞腫に関する論文数の経年的変化  
(PubMed. <http://www.ncbi.nlm.nih.gov/pubmed/>より算出)

\* Present situation and problems in the clinical practice and research of pheochromocytoma.

\*\* Mitsuhide NARUSE, M.D., Ph.D.: 国立病院機構京都医療センター臨床研究センター内分泌代謝高血圧研究部 [〒612-8555 京都市伏見区深草向畑町1-1]; Department of Endocrinology, Metabolism, and Hypertension, Clinical Research Institute, National Hospital Organization, Kyoto Medical Center, Kyoto 612-8555, JAPAN

\*\*\* Milka TSUIKI, M.D., Ph.D. & Akiyo TANABE, M.D., Ph.D.: 東京女子医科大学第二内科

表 1 褐色細胞腫の臨床的課題

1. 悪性腫瘍の頻度が高い
2. 初回手術時の良性、悪性診断が困難
3. 悪性例では後年になり遠隔転移
4. 働き盛りに多く罹病期間が長い
5. 診断後の治療法が未確立

国疫学調査<sup>10)</sup>では、一次調査における褐色細胞腫の患者数は522例、推定患者数は約1,000例で2次調査での悪性褐色細胞腫の頻度は10.8%であると推測されている。原発性アルドステロン症では0.2%、クッシング症候群では1.2%が悪性で、褐色細胞腫は内分泌腫瘍のなかでも悪性の頻度が最も高い腫瘍と言える(図2)。

## 2. 第二の課題

初回診断時に良性か悪性かを鑑別するのがきわめて困難なことである。多発性転移があれば診断は容易であるが、一側副腎の単発性腫瘍の場合、組織学的にそれを悪性と診断することはきわめて難しい。多くは良性と診断され、術後、血圧、カテコラミンが正常化し、治癒と診断されるが、数年後に骨転移などの遠隔転移が発見され悪性であったことが判明することが少なくない。東京女子医科大学の田辺らは、悪性褐色細胞腫の自験例の約80%は初回診断時には良性と診断されていたと報告している。

## 3. 第三の課題

局所再発に加えて多発性の遠隔転移が多いことで、骨転移が最も多く約70%に認められ、その他約40%に肺、肝、腹腔内リンパ節への転移を認める。遠隔転移の頻度が高いことが外科的治療を困難にしており、全身治療が必要となる。

## 4. 第四の課題

20歳の後半から40歳ぐらいの比較的若年者に多く、約60%を占める。しかも数年の経過で徐々に、しかし進行性に増悪するため、その間患

者は身体的のみならず仕事や家庭面で社会的、経済的、心理的に大きな負担を抱えた生活を余儀なくされる。田辺らの検討では、褐色細胞腫は初発症状から1~2年で診断され、腫瘍が発見されて初回手術を受けるが、悪性例ではその後平均5年で転移、再発を認め、その後平均7年で死亡する(図3)。初回手術後25年とのきわめて長期になる例もあり、患者と家族の負担がきわめて大きい。

## 5. 第五の課題

悪性と診断されても有効な治療法は未確立である。実際には手術、化学療法、MIBG治療などの多様な治療を組み合わせ、反復、継続する必要があるが、有効性は十分には検証されておらず、また、MIBG治療は保険適応になっていない。

このようなことから、悪性褐色細胞腫は明らかに内分泌領域における代表的な難治性疾患であるが、これまでの取り組みは十分とは言えない。

## 診療水準向上における課題(表2)

本疾患の診療水準向上に際して解決すべき課題を表2にまとめた。

### 1. 第一の課題

まず、最大の要因は本疾患に対して必ずしも専門医の関心が高くない点である。カテコラミン測定法とCT, MRIなどの画像診断法の進歩により、典型的な褐色細胞腫の診断が容易となり、内視鏡的手術による治療も確立されたとも言える。コルチゾール、アルドステロンなどのステロイドの研究、副腎皮質疾患の専門医と比較すると、カテコラミンの研究、褐色細胞腫の専門医師はきわめて少ない。褐色細胞腫の診断、治療法の確立はこの傾向をさらに助長してきたと言える。今後、専門の研究者、臨床医の増加は診療水準向上に不可欠である。

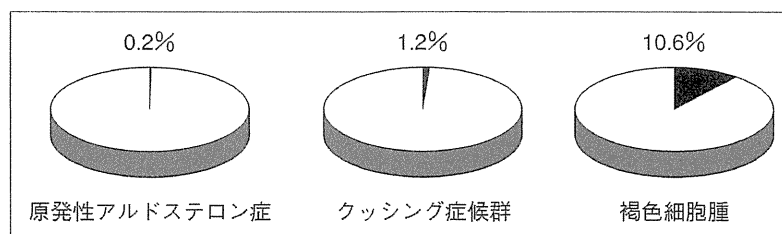


図2 代表的な副腎性高血圧症における悪性腫瘍の頻度(文献<sup>10)</sup>より引用)

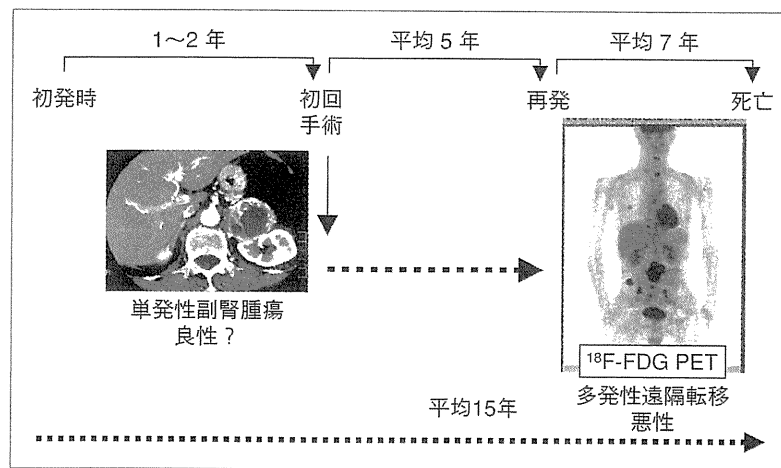


図3 悪性褐色細胞腫の典型的な臨床経過(文献<sup>3)7)9)</sup>より引用)

表2 診療水準向上に際して改善すべき課題

1. 関心の高い研究者、臨床医の減少
2. 内科を経由しないで手術される症例の増加
3. 厚生労働省の特定疾患に含まれていない
4. 本邦における(悪性)褐色細胞腫の実態が不明
5. 疾患の診療情報を共有するシステム未確立

## 2. 第二の課題

内科での経験例が減少していることがあげられる。原発性アルドステロン症とは対照的に腫瘍が大きいことから、泌尿器科、外科に直接紹介され手術される例が多いと推測される。東京女子医科大学第二内科でも、現在著者が所属する京都医療センターでも、従来と比較して、'褐色細胞腫'の経験例はきわめて少なくなっている。

## 3. 第三の課題

褐色細胞腫が厚生労働省の難病指定となっておらず、特定疾患副腎ホルモン産生異常症調査研究班の調査、研究対象ともなっていない点である。良性褐色細胞腫の診断、治療法の確立に伴い、難病である悪性褐色細胞腫が取り残された状況になり、本疾患の系統的研究を困難にしている。

## 4. 第四の課題

褐色細胞腫、悪性褐色細胞腫の実態が明らかでない点である。1998年の厚生労働省研究会議の調査以降、全国疫学調査が実施されておらず、患者数、診療状況、予後など、有効な対策を立てる疫学情報がほとんどない。

## 5. 第五の課題

診断法、治療法に関するエビデンス構築には、

長期的な視点に立った診療情報の収集システム確立が不可欠であるが未確立である。特に、初回診断後25年も経て遠隔転移を示す例があることから、疾患レジストリーが必要である。

このような背景から、褐色細胞腫の症例を経験した場合に、どのような点に注意して検査を行い、術後経過観察するのか、また、悪性であることが明らかな症例を経験した場合に、何をどこまで検査すべきか、どのような治療の選択肢があるのかなど十分な情報がなく、手探りの診療になっているのが現状である。

## 改善の方策

このような現状を改善するために何が必要であるか、望まれる対策は4点ある。

### 1. 第一の対策

全国実態調査である。悪性を早期に診断するとの観点から、悪性褐色細胞腫のみならずすべての褐色細胞腫を対象とする必要がある。このため、内科のみならず、本疾患の診療に従事する泌尿器科、内分泌外科などの関連分野も対象とする必要がある。

### 2. 第二の対策

悪性マーカーの共同解析体制の整備である。

#### (1) 病理組織所見マーカー

これまで、手術時の病理組織所見からは悪性の診断が困難であるとされてきた。しかしながら最近、Thompsonら<sup>11)</sup>、Kimuraら<sup>12)</sup>は独自のスコアリング方法を考案し、分化型、低分化型の鑑別、

表 3 未発症保因者に対する臨床的対応案

|  |
|--|
| 1. 遺伝性褐色細胞腫・パラグングリオーマ症候群をよく理解した臨床内分泌専門医により行われるべきである。 |
| 2. 定期的フォローアップ  |
| 1) 対象：家系内の最も若年発症者の発症年齢から10年を引いた年齢から                  |
| 2) 検査：(1) 内科的診察・尿中メタネフリン測定：毎年                        |
| (2) CTあるいはMRI：2年に1回                                  |
| (3) MIBGシンチ：3年に1回                                    |

(文献<sup>17)</sup>より引用，一部改変)

表 4 褐色細胞腫における遺伝子解析に関する見解(要点)

褐色細胞腫患者におけるSDHB遺伝子変異解析は、患者予後の予測、適切な治療による予後改善に有益である可能性が示唆される一方、効果的な診断・治療法は未確立である。変異が同定された患者の血縁者における解析も、変異陽性の場合、早期の診断・治療により予後改善に有益である可能性があるが、遺伝子型と表現型との関連や効果的な早期発見・治療法は確立されていない。すなわち、現時点では、褐色細胞腫におけるSDHB遺伝子解析は臨床的有用性が確立しておらず、遺伝子診断ではなく、遺伝子解析研究と位置づけられる。患者あるいはその血縁者において遺伝子解析を実施する場合は、その意義と限界・予想される問題を十分に認識し、「ヒトゲノム・遺伝子解析に関する倫理指針」を遵守するとともに、前述の実施の必要条件を十分に確認することが推奨され、また、これらの条件は実施の十分条件でない可能性も考慮する必要がある。特に、血縁者においては臨床的意義が未確立であることから、現時点では解析の実施はきわめて慎重に行われるべきである。一方、SDHB遺伝子変異は悪性褐色細胞腫の早期診断マーカーとして期待されていることから、整備され、責任ある実施環境下で、統一的、系統的な多施設共同研究として推進されることが重要と考えられる。

(日本内分泌学会。http://square.umin.ac.jp/endocrine/より引用)

予後予測に有用であることを報告している。各施設の病理医と内分泌病理専門医との連携により、臨床所見と組織解析結果との比較対応を行い、データを蓄積していく体制の整備が必要である。これには日本内分泌学会、日本内分泌病理学会などの関連学会の協力体制が必要である。

#### (2) 遺伝子変異マーカー

最近、サクシニル酸脱水素酵素の遺伝子、特にSDHBの変異との関連を示唆する結果が諸外国から報告されている<sup>13)14)</sup>。わが国でも筑波大学の竹越らが、その遺伝子解析の有用性を積極的に検討している。悪性褐色細胞腫の約35%がSDHB遺伝子変異陽性である一方、褐色細胞腫でSDHB遺伝子変異陽性例の約20~30%が後年悪性化を示すとの報告<sup>15)</sup>もある。また、すでに悪性褐色細胞腫と診断された患者でSDHB遺伝子変異陽性は患者の予後を予測するとの報告<sup>16)</sup>もある。それゆえ、これらの遺伝子変異は悪性褐色細胞腫の有用な診断マーカーになることが期待される。

陽性の場合、原発腫瘍の手術後であっても長期にわたり十分な経過観察が望ましい。しかし、何を指標としてどの程度の間隔で、いつまで検査すべきか確立されていない。さらに陽性例と陰性例

の予後の差や血縁者での解析の臨床的意義も確立されていない。米国ではSDHB変異陽性無症候性キャリアーの家族会も結成されているが、わが国では文化や社会的背景が大きく異なる。解析をするメリットに加えて随伴する種々の課題を十分に考慮し、得られた結果を責任を持って経過観察し、診断、治療に反映させていく姿勢と医療体制の充実が必要といえる。表3にYoungら<sup>17)</sup>による無症候性キャリアーの経過観察指針を示す。また、本疾患における遺伝子解析に関して、日本内分泌学会悪性褐色細胞腫検討委員会において「遺伝子変異解析に関する見解」を作成し、内分泌学会ホームページに掲載している(表4)。

#### 3. 第三の対策

治療法の有効性に関する客観的評価体制の確立とエビデンスの構築である。血圧コントロールには主にαブロッカーを投与するが、血圧コントロールが不十分な例では、カテコラミン合成酵素阻害薬であるパラメチルトイロシン(デムサ®)の投与も併用されることがある。しかしながら、国内未承認薬であり、患者の個人輸入が必要で、使用に際しては倫理委員会での承認が望ましい。

化学療法としてはCVD併用化学療法が代表的で

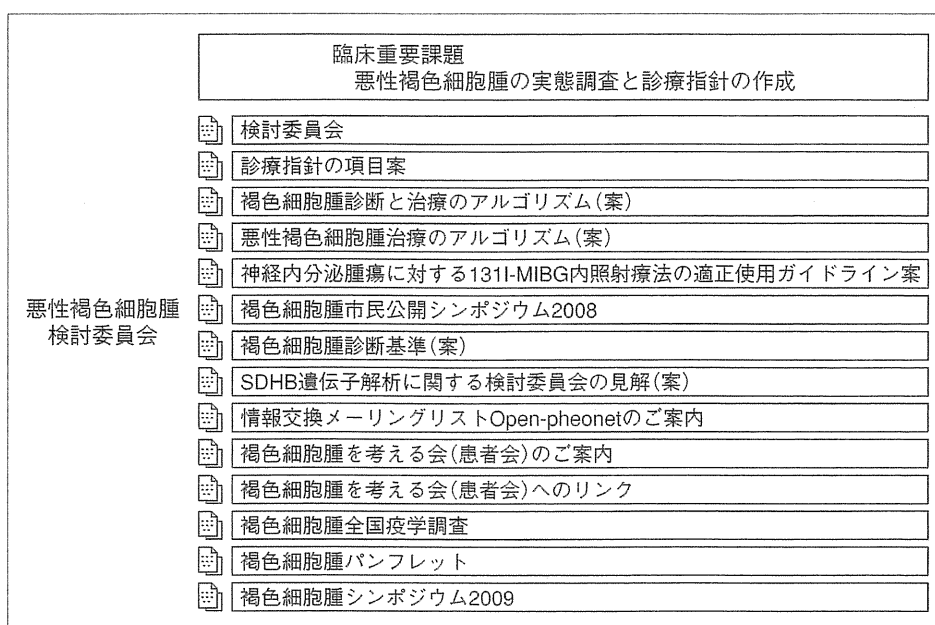


図4 日本内分泌学会検討委員会による悪性褐色細胞腫に対する取り組み  
(日本内分泌学会. [http://square.umin.ac.jp/endocrine/rinsho\\_juyo/index.html](http://square.umin.ac.jp/endocrine/rinsho_juyo/index.html)より引用)

ある。Averbuchら<sup>18)</sup>は、平均21か月の観察期間で、腫瘍の完全あるいは部分奏効は57%、ホルモンの完全あるいは部分奏効は79%に認められたと報告しているが、その後、その有効性についての客観的エビデンスの報告はない。ランダム化比較試験の実施が望ましいが、患者が複数の施設に分散しており、個々の患者の臨床背景にきわめて大きな差があるため、実施は容易ではない。今後、多施設共同により、少なくとも非ランダム化比較試験などによる有効性に関するエビデンスの構築が必要である。また、最も有効性が期待されているのはMIBGシンチ陽性例でのMIBG治療で、諸外国では多数の症例で実施されている。しかしわが国では保険適応となっておらず、これまで金沢大学、群馬大学、北海道大学の核医学教室で実施されてきたにとどまる。最近、日本核医学会からMIBG内照射療法に関するガイドライン(案)が提案されている。今後、その適応や治療成績などについて、内科と核医学との連携強化が必要である。

#### 4. 第四の対策

臨床共同研究(疫学研究、臨床研究)の実施や診療情報の共有が可能な施設間ネットワーク、疾患レジストリーの基盤構築である。診断、治療成績の評価、長期予後の評価などは、限られ

た施設の限られた医師、研究者のみでは到底実行不可能である。近年、癌登録も始まっており、また、インターネットのWEBを活用した疾患登録も広まりつつある。今後、倫理面にも十分に配慮しながら、患者の動向、動態や予後を長期にみていく体制作りが必要である。

#### これまでの取り組みと現状

このような多面的な活動を進めるには、なんらかの組織が必要で、米国のPRESSORが一つのモデルになると考えられる。しかし、国ごとに事情は異なることから、やはりわが国独自の組織が望ましく、その上で、海外の組織と連携していくのがよいと言える。著者らは、悪性褐色細胞腫の診療に従事する関連診療科の医師とともに、「PHEOワーキンググループ」を作り、「悪性褐色細胞腫シンポジウム」(国立病院機構京都医療センター主催、2007年1月20日(土)、東京国際フォーラム)やワーキンググループ打ち合わせ会などを開催してきたが、2007年からは日本内分泌学会臨床重要課題([http://square.umin.ac.jp/endocrine/rinsho\\_juyo/index.html](http://square.umin.ac.jp/endocrine/rinsho_juyo/index.html))として、検討委員会として図4に上げた種々の活動と情報提供を行っている。そのなかには、全国

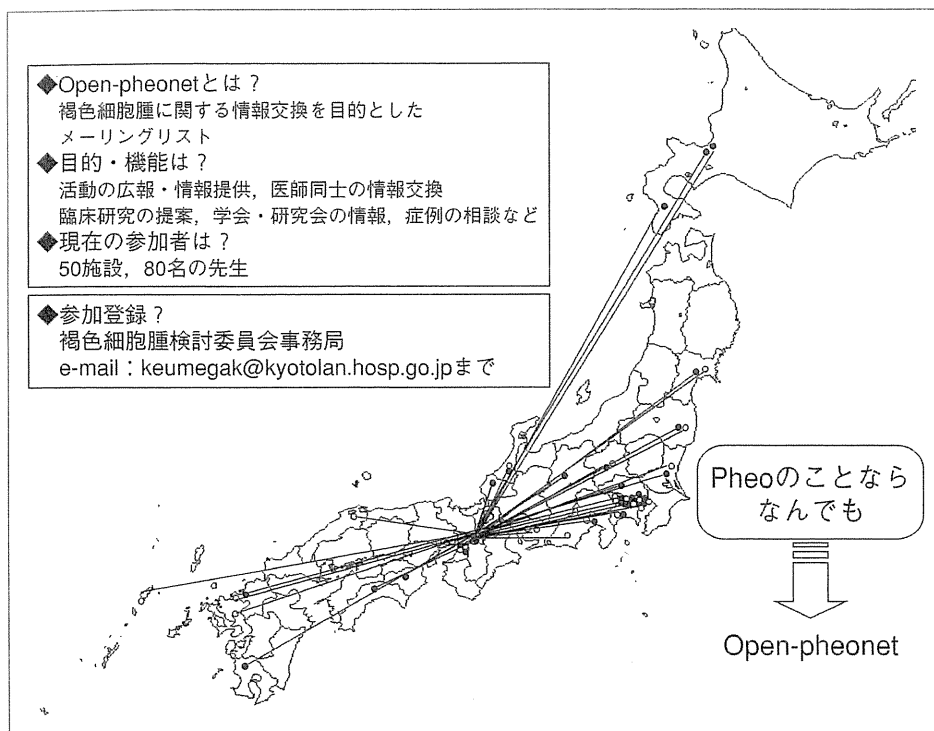


図5 Open-pheonetnetworkの目的, 機能, 現状

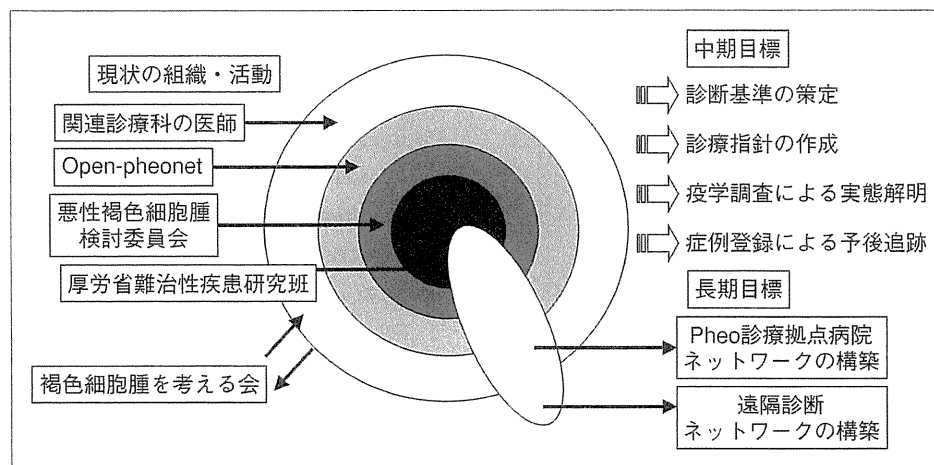


図6 褐色細胞腫診療水準向上のための組織, 活動, 中・長期目標

の医師向けの情報交換メーリングリストである open-pheonetの立ち上げもある。実際の症例の診断, 治療に関する情報収集, 臨床研究の提案・実施, 学会や厚生労働省班会議の情報提供など, 多目的情報ネットワークである。現在, 全国で約80名の先生が参加され活用されている(図5)。

さらに2009年には厚生労働省難治性疾患克服事業の調査奨励研究として, 全国疫学調査を実

施, 一次調査約65%, 二次調査約85%の回収率を得て, 褐色細胞腫の推定患者数が約3,000名, そのうち約10%が悪性褐色細胞腫であることを明らかにした。現在, 調査結果のまとめと診療指針の刊行に向けて準備中である。さらに次年度以降, 本研究班の継続を予定しており, 疾患登録, 遺伝子解析, 病理診断の集中解析と予後追跡体制の基盤を確立する予定である。



## まとめ

悪性褐色細胞腫は内分泌分野における難治性疾患の代表である。遠隔転移を認めない褐色細胞腫が‘良性’であることを示す確実な方法はない。その意味で、褐色細胞腫を経験したとしてもかく‘悪性の可能性を考える’必要がある。悪性褐色細胞腫の患者を担当すると、たちまち治療方針に難渋するのが現状である。図6にこれまでの組織、活動および中期的、長期的目標を図示した。現在、中期目標を達成しつつあるが、今後さらに関連学会、基幹施設との協力により、褐色細胞腫診療拠点ネットワークや専門医による遠隔診断ネットワークの構築が期待され、それを通じて早期診断法、有効な治療法の確立、長期予後の解明などが可能になると考えられる。

## 文 献

- 1) 成瀬光栄, 田辺晶代, 長田太助, ほか. 褐色細胞腫の診断における問題点. 血圧 2005 ; 12 : 765.
- 2) 成瀬光栄, 田辺晶代, 長田太助, ほか. 副腎髄質. 金澤康徳, 武谷雄二, 関原久彦, ほか・編. Annual Review内分泌, 代謝2005. 東京 : 中外医学社 ; 2005. p. 237.
- 3) 田辺晶代, 立木美香, 成瀬光栄, ほか. 悪性褐色細胞腫. 別冊 新領域別症候群シリーズ. 内分泌症候群(第2版)I—その他の内分泌疾患を含めて—. 2006. p. 739.
- 4) 成瀬光栄. 褐色細胞腫診療の問題点—悪性度の診断. 金澤康徳, 武谷雄二, 関原久彦, ほか・編. Annual Review糖尿病・代謝・内分泌 2006. 東京 : 中外医学社 ; 2006. p. 206.
- 5) 成瀬光栄, 田辺晶代. 褐色細胞腫の診断と治療 update. 日内会誌 2006 ; 95 : 650.
- 6) 成瀬光栄, 田辺晶代. 高血圧クリーゼ/褐色細胞腫. 救急・集中治療 2006 ; 18 : 1099.
- 7) 成瀬光栄, 田辺晶代. 褐色細胞腫の診断と治療. 血圧 2007 ; 14 : 721.
- 8) 成瀬光栄. 内分泌代謝専門医ガイドブック. 成瀬光栄, 平田結喜緒, 島津 章・編. 東京 : 診断と治療社 ; 2007. p. 172.
- 9) 田辺晶代, 立木美香, 渡辺大輔, ほか. 褐色細胞腫. Heart View 2007 ; 95 : 29.
- 10) 名和田 新. 副腎ホルモン産生異常症の全国疫学調査. 厚生省特定疾患「副腎ホルモン産生異常症」調査研究班, 平成10年度研究報告書. 1999.
- 11) Thompson LD. Pheochromocytoma of the Adrenal gland Scaled Score (PASS) to separate benign from malignant neoplasms : a clinicopathologic and immunophenotypic study of 100 cases. Am J Surg Pathol 2002 ; 26 : 551.
- 12) Kimura N, Watanabe T, Noshiro T, et al. Histological grading of adrenal and extra-adrenal pheochromocytomas and relationship to prognosis : a clinicopathological analysis of 116 adrenal pheochromocytomas and 30 extra-adrenal sympathetic paragangliomas including 38 malignant tumors. Endocrine Pathology 2005 ; 16 : 23.
- 13) Neumann HP, Cybulla M, Shibata H, et al. New genetic causes of pheochromocytoma : current concepts and the clinical relevance. Keio J Med 2005 ; 54 : 15.
- 14) Gimenez-Roqueplo AP, Lehnert H, Mannelli M, et al. Pheochromocytoma, new genes and screening strategies. Clin Endocrinol (Oxf) 2006 ; 65 : 699.
- 15) Benn DE, Gimenez-Roqueplo AP, Reilly JR, et al. Clinical presentation and penetrance of pheochromocytoma/paraganglioma syndromes. J Clin Endocrinol Metab 2006 ; 91 : 827.
- 16) Amar L, Baudin E, Burnichon N, et al. Succinate dehydrogenase B gene mutations predict survival in patients with malignant pheochromocytomas or paragangliomas. J Clin Endocrinol Metab 2007 ; 92 : 3822.
- 17) Young WF Jr. Adrenal causes of hypertension : pheochromocytoma and primary aldosteronism. Endocr Metab Disord 2007 ; 8 : 309.
- 18) Averbuch SD, Steakley CS, Young RC, et al. Malignant pheochromocytoma : effective treatment with a combination of cyclophosphamide, vincristine, and dacarbazine. Ann Intern Med 1988 ; 109 : 267.

\* \* \*

Original article

# Low-dose $^{123}\text{I}$ -metaiodobenzylguanidine diagnostic scan is inferior to $^{131}\text{I}$ -metaiodobenzylguanidine posttreatment scan in detection of malignant pheochromocytoma and paraganglioma

Daiki Kayano, Junichi Taki, Makoto Fukuoka, Hiroshi Wakabayashi, Anri Inaki, Ayane Nakamura and Seigo Kinuya

**Objective** We assessed the lesion detectability of low-dose diagnostic  $^{123}\text{I}$ -metaiodobenzylguanidine (MIBG) whole-body scans obtained at 6 and 24 h compared with posttreatment  $^{131}\text{I}$ -MIBG whole-body scans in malignant pheochromocytoma and paraganglioma.

**Methods** Scintigrams obtained in 15 patients with malignant pheochromocytoma and paraganglioma were retrospectively analyzed. Diagnostic scans were performed with 111 MBq of  $^{123}\text{I}$ -MIBG. Therapeutic doses of  $^{131}\text{I}$ -MIBG (5.55–7.40 GBq) were administered and whole-body scans were obtained at 2–5 days after  $^{131}\text{I}$ -MIBG administrations. We compared the number of lesions and the lesion-to-referent count ratios at 6 and 24 h of  $^{123}\text{I}$ -MIBG and at 2–5 days of  $^{131}\text{I}$ -MIBG.

**Results** In comparison with the 6-h images of  $^{123}\text{I}$ -MIBG, the 24-h images of  $^{123}\text{I}$ -MIBG could detect more lesions in eight patients. Posttreatment  $^{131}\text{I}$ -MIBG scans revealed new lesions in eight patients compared with the 24-h images of  $^{123}\text{I}$ -MIBG. The lesion-to-referent count ratios at 6 and 24 h of  $^{123}\text{I}$ -MIBG and at 3 days of  $^{131}\text{I}$ -MIBG were increasing at later scanning time. There were significant

differences in the lesion-to-referent count ratios between 6 and 24 h of  $^{123}\text{I}$ -MIBG ( $P = 0.031$ ), 6 h of  $^{123}\text{I}$ -MIBG and 3 days of  $^{131}\text{I}$ -MIBG ( $P = 0.020$ ), and 24 h of  $^{123}\text{I}$ -MIBG and 3 days of  $^{131}\text{I}$ -MIBG ( $P = 0.018$ ).

**Conclusion** Low-dose diagnostic  $^{123}\text{I}$ -MIBG whole-body scan is inferior to posttreatment  $^{131}\text{I}$ -MIBG whole-body scan in malignant pheochromocytoma and paraganglioma. Considering the scan timing of  $^{123}\text{I}$ -MIBG, 6-h images might have no superiority compared with 24-h images. *Nucl Med Commun* 32:941–946 © 2011 Wolters Kluwer Health | Lippincott Williams & Wilkins.

Nuclear Medicine Communications 2011, 32:941–946

**Keywords:**  $^{123}\text{I}$ ,  $^{131}\text{I}$ , pheochromocytoma, paraganglioma, metaiodobenzylguanidine

Department of Nuclear Medicine, Kanazawa University Hospital, Kanazawa, Ishikawa, Japan

Correspondence Daiki Kayano, Department of Nuclear Medicine, Kanazawa University Hospital, 13-1 Takara-machi, Kanazawa, Ishikawa 920 8641, Japan  
Tel: +81 76 265 2333; fax: +81 76 234 4257;  
e-mail: kayano@nmd.m.kanazawa-u.ac.jp

Received 23 May 2011 Revised 23 June 2011 Accepted 25 June 2011

## Introduction

Metaiodobenzylguanidine (MIBG), which can be labeled with either  $^{131}\text{I}$  or  $^{123}\text{I}$ , mimics the neurotransmitter norepinephrine and specifically targets malignant cells of the sympathetic nervous system [1,2]. Since  $^{131}\text{I}$ -MIBG was reported to visualize tumors of the adrenal medulla in the early 1980s [3,4],  $^{131}\text{I}$ -MIBG and  $^{123}\text{I}$ -MIBG have been widely used for detecting lesions in patients with malignant neuroendocrine tumors, such as malignant pheochromocytomas, malignant paragangliomas, medullary thyroid carcinomas, carcinoid tumors, and neuroblastomas [5–9].  $^{123}\text{I}$ -MIBG has superiority over  $^{131}\text{I}$ -MIBG with diagnostic use, because the  $\gamma$ -ray energy of  $^{123}\text{I}$  (159 keV) befits the image quality and lesion detectability for scintigraphy compared with that of  $^{131}\text{I}$  (364 keV) [10–12]. Moreover,  $^{123}\text{I}$  offers favorable dosimetry compared with  $^{131}\text{I}$  because of their  $\gamma$ -ray energies and their half-lives ( $^{123}\text{I}$ : 13.13 h,  $^{131}\text{I}$ : 8.04 days) [13].

It has been reported that other imaging modalities may be useful in detecting neuroendocrine tumors. Many

studies that compared  $^{123}\text{I}$ -MIBG with  $^{18}\text{F}$ -fluoro-2-deoxy-D-glucose ( $^{18}\text{F}$ -FDG) positron emission tomography (PET) or  $^{18}\text{F}$ -FDG PET/computed tomography (CT) have been reported. These studies did not show good concordance [14–17], and therefore  $^{123}\text{I}$ -MIBG and  $^{18}\text{F}$ -FDG PET would possess complementary roles.  $^{18}\text{F}$ -3,4-dihydroxy-phenylalanine PET,  $^{18}\text{F}$ -fluorodopamine PET, and  $^{68}\text{Ga}$ -DOTA peptides PET might be preferred in comparison with  $^{123}\text{I}$ -MIBG [17,18]. However, the evidence for these radiopharmaceuticals is insufficient and these have not become widely used yet.

As a prelude to  $^{131}\text{I}$ -MIBG therapy,  $^{123}\text{I}$ -MIBG scintigraphy is essential for the confirmation of MIBG accumulation to lesions. After  $^{131}\text{I}$ -MIBG therapy, posttreatment  $^{131}\text{I}$ -MIBG scintigraphy is routinely used to assess tumor uptake rather than lesion detectability. Lesional detectability of  $^{123}\text{I}$ -MIBG scans was not always the same as that of posttreatment  $^{131}\text{I}$ -MIBG scans. Campbell *et al.* [19] reported a case in which the posttreatment  $^{131}\text{I}$ -MIBG image depicted more metastatic lesions compared with the  $^{131}\text{I}$ -MIBG

Table 1 Clinical characteristics and protocol of  $^{131}\text{I}$ -metaiodobenzylguanidine therapy

| Patient number | Age | Sex    | Diagnosis                  | $^{131}\text{I}$ -MIBG |                      |
|----------------|-----|--------|----------------------------|------------------------|----------------------|
|                |     |        |                            | Dose (GBq)             | Scanning time (days) |
| 1              | 43  | Male   | Malignant pheochromocytoma | 7.4                    | 5                    |
| 2              | 46  | Male   | Malignant paraganglioma    | 7.4                    | 5                    |
| 3              | 78  | Female | Malignant pheochromocytoma | 7.4                    | 3                    |
| 4              | 76  | Male   | Malignant pheochromocytoma | 7.4                    | 4                    |
| 5              | 52  | Male   | Malignant pheochromocytoma | 7.4                    | 5                    |
| 6              | 63  | Male   | Malignant pheochromocytoma | 7.4                    | 3                    |
| 7              | 45  | Male   | Malignant pheochromocytoma | 7.4                    | 3                    |
| 8              | 75  | Male   | Malignant pheochromocytoma | 5.55                   | 2                    |
| 9              | 61  | Male   | Malignant paraganglioma    | 7.4                    | 3                    |
| 10             | 69  | Male   | Malignant pheochromocytoma | 7.4                    | 3                    |
| 11             | 60  | Female | Malignant pheochromocytoma | 7.4                    | 3                    |
| 12             | 37  | Female | Malignant pheochromocytoma | 7.4                    | 3                    |
| 13             | 54  | Female | Malignant paraganglioma    | 7.4                    | 3                    |
| 14             | 39  | Female | Malignant pheochromocytoma | 7.4                    | 3                    |
| 15             | 58  | Female | Malignant pheochromocytoma | 7.4                    | 3                    |

MIBG, metaiodobenzylguanidine.

diagnostic scan and  $^{123}\text{I}$ -MIBG scan in a patient with malignant pheochromocytoma. Fukuoka *et al.* [20] demonstrated that 3-day images of posttherapeutic  $^{131}\text{I}$ -MIBG had superiority over 6-h images of low-dose diagnostic  $^{123}\text{I}$ -MIBG in patients with malignant pheochromocytomas, malignant paragangliomas, and neuroblastomas. Considering the lesion-to-background count ratios of  $^{123}\text{I}$ -MIBG images, 6-h images would be inferior to 24-h images in detecting lesions. To our knowledge, most previous studies evaluated scintigrams only by visual assessment, and there is no literature that reports the quantitative analysis of the image based on the count density and the lesion detectability between 6 and 24-h scans of diagnostic  $^{123}\text{I}$ -MIBG and posttherapeutic  $^{131}\text{I}$ -MIBG scans.

In this study, we compared low-dose diagnostic  $^{123}\text{I}$ -MIBG scans obtained at 6 h, at 24 h, and posttreatment  $^{131}\text{I}$ -MIBG scans by visual and quantitative methods in detecting lesions of malignant pheochromocytoma and paraganglioma; we then evaluated the validity of the dose and the scanning time of  $^{123}\text{I}$ -MIBG scintigraphy.

## Methods

### Patients

We studied 15 consecutive patients who underwent first  $^{131}\text{I}$ -MIBG therapy for adult malignant pheochromocytoma and paraganglioma between March 2005 and 2010. The patients consisted of nine men and six women, and the age range was 37–78 years (mean = 57.1 years). Twelve had malignant pheochromocytomas and three patients had malignant paragangliomas (Table 1). In all patients, we confirmed MIBG accumulations in the primary or metastatic lesions with diagnostic  $^{123}\text{I}$ -MIBG scintigraphy before  $^{131}\text{I}$ -MIBG therapy.

### Low-dose diagnostic $^{123}\text{I}$ -metaiodobenzylguanidine scintigraphy

We performed  $^{123}\text{I}$ -MIBG scintigraphy after intravenous injection of 111 MBq of  $^{123}\text{I}$ -MIBG (Fujifilm RI Pharma Co., Ltd., Japan), using a dual-head gamma camera equip-

ped with a low-medium-energy general-purpose collimator (Toshiba E-cam, Tokyo, Japan or Siemens Medical Solutions, Symbia, Germany), specifically designed for reduced scatter and septal penetration of the small fraction of  $^{123}\text{I}$  high-energy photons. The activity of  $^{123}\text{I}$ -MIBG was assayed by the supplier to become 111 MBq at noon of the administration day. In this study, the dose of  $^{123}\text{I}$ -MIBG was relatively low compared with the standard dose of  $^{123}\text{I}$ -MIBG in Western countries, which was approved up to 400 MBq [13,21], as only 111 MBq of  $^{123}\text{I}$ -MIBG had been available for adults due to Japanese regulations until October 2010. Whole-body scans were obtained at 6 and 24 h after  $^{123}\text{I}$ -MIBG administration with 15 cm/min of scanning speed on a photo peak of 159 keV with a 15% window.

### $^{131}\text{I}$ -metaiodobenzylguanidine therapy and posttherapeutic scintigraphy

$^{131}\text{I}$ -MIBG therapy was performed 2–21 days (mean = 11.9 days) after diagnostic  $^{123}\text{I}$ -MIBG scintigraphy. To prevent thyroidal uptake of free iodine, oral administration of 200 mg of potassium iodide was commenced, 1 day before  $^{131}\text{I}$ -MIBG administration and continued for up to 10 days posttherapy. We intravenously administered 5.55–7.4 GBq (mean = 7.28 GBq) of  $^{131}\text{I}$ -MIBG through fixed peripheral venous lines for approximately an hour using a lead-shielded infusion pump with monitoring vital signs for more than 6 h from the beginning of  $^{131}\text{I}$ -MIBG administration. All patients were treated in the isolation room until radiation decreased to less than 30  $\mu\text{Sv/h}$  at 1 m. All therapies were well tolerated. A whole-body scan with therapeutic dose of  $^{131}\text{I}$ -MIBG was obtained once at 2–5 days (mean = 3.4 days) after injection with 15 cm/min of scanning speed on a photo peak of 364 keV with a 15% window, using a high-energy collimator. Table 1 shows the dosage and the scanning time of  $^{131}\text{I}$ -MIBG therapy.

### Visual evaluation

Two experienced nuclear medicine physicians of our institution, who were blinded to the findings of the other

imaging modalities, evaluated the accumulations of 6 and 24-h images of <sup>123</sup>I-MIBG and a posttreatment <sup>131</sup>I-MIBG image. They interpreted all foci except for physiological accumulation as abnormal uptake and defined their anatomical location. Diffuse accumulation at nasal cavity, salivary glands, thyroid, myocardium, liver, and bladder were considered as physiological uptake. When small lesions or low MIBG uptake lesions are overlapped with physiological (e.g. liver) uptake, some lesions might be undetected. When their interpretation was discordant, they obtained consensus after conference. To compare the lesion detectability of 6- and 24-h images of <sup>123</sup>I-MIBG with a posttreatment <sup>131</sup>I-MIBG image, we investigated the difference in the number of detected lesions in the following four sites: bone, lungs, liver, and others.

**Quantitative evaluation**

As a quantitative evaluation, we used the uptake ratio. On anterior and posterior images at 24 h of <sup>123</sup>I-MIBG, a target region of interest (ROI) was set manually by tracing the margin of the most intense lesion and a referential ROI and a background ROI were set on the left thigh and the background. The same ROIs were used on each image at 6 h of <sup>123</sup>I-MIBG and at 3 days of <sup>131</sup>I-MIBG. In cases in which metastatic lesions existed in the left thigh, the right thigh was used as a referential ROI. The uptake ratio was calculated with each mean ROI count by the following formula: uptake ratio = (target ROI – background ROI)/(referential ROI – background ROI). We compared the uptake ratios at 6 and 24 h of <sup>123</sup>I-MIBG and at 3 days of <sup>131</sup>I-MIBG. To standardize the scanning time, we evaluated 10 patients whose <sup>131</sup>I-MIBG scans were obtained at 3 days after <sup>131</sup>I-MIBG therapeutics.

**Statistical analysis**

The paired *t*-test was used for the analysis of the sequential changes of the uptake ratios between 6 and 24 h after <sup>123</sup>I-MIBG injections and 3 days after <sup>131</sup>I-MIBG administrations. A *P* value of less than 0.05 was considered as a significant difference.

**Results**

A total of 96 and 106 lesions were identified with 6- and 24-h images of <sup>123</sup>I-MIBG, respectively. <sup>131</sup>I-MIBG posttreatment scans detected 170 lesions. Table 2 summarizes visual analyses. In comparison with the 6-h images of <sup>123</sup>I-MIBG, the 24-h images of <sup>123</sup>I-MIBG could detect more lesions in eight (53%) of 15 patients. In all patients, the 6-h images of <sup>123</sup>I-MIBG had no advantage compared with the 24-h images of <sup>123</sup>I-MIBG in detecting lesions. In comparison between diagnostic <sup>123</sup>I-MIBG scans and posttreatment <sup>131</sup>I-MIBG scans, posttreatment <sup>131</sup>I-MIBG scans had better lesional detectability than diagnostic <sup>123</sup>I-MIBG scans in eight (53%) of 15 patients. <sup>123</sup>I-MIBG scans were not superior to <sup>131</sup>I-MIBG scans in any cases. Table 3 shows the number of detected lesions in bone, lungs, liver, and

**Table 2** The number of lesions on diagnostic <sup>123</sup>I-metaiodobenzylguanidine scans (6 and 24 h) and posttreatment <sup>131</sup>I-metaiodobenzylguanidine scans (2–5 days)

| Patient number | <sup>123</sup> I-MIBG |      | <sup>131</sup> I-MIBG |
|----------------|-----------------------|------|-----------------------|
|                | 6 h                   | 24 h | 2–5 days              |
| 1              | 9                     | 10   | 10                    |
| 2              | 5                     | 5    | 5                     |
| 3              | 7                     | 7    | 14                    |
| 4              | 10                    | 10   | 13                    |
| 5              | 1                     | 1    | 1                     |
| 6              | 3                     | 3    | 9                     |
| 7              | 5                     | 6    | 6                     |
| 8              | 3                     | 4    | 6                     |
| 9              | 23                    | 24   | 45                    |
| 10             | 1                     | 2    | 2                     |
| 11             | 6                     | 6    | 6                     |
| 12             | 0                     | 1    | 1                     |
| 13             | 1                     | 1    | 4                     |
| 14             | 6                     | 9    | 17                    |
| 15             | 16                    | 17   | 31                    |
| Total          | 96                    | 106  | 170                   |

MIBG, metaiodobenzylguanidine.

**Table 3** The number of lesions detected in bone, lung, liver, and others with diagnostic <sup>123</sup>I-metaiodobenzylguanidine scans and posttreatment <sup>131</sup>I-metaiodobenzylguanidine scans

|                                | Bone | Lung | Liver | Others | Total |
|--------------------------------|------|------|-------|--------|-------|
| <sup>123</sup> I-MIBG scan (n) | 64   | 9    | 15    | 18     | 106   |
| <sup>131</sup> I-MIBG scan (n) | 115  | 14   | 17    | 24     | 170   |

MIBG, metaiodobenzylguanidine.

others with diagnostic <sup>123</sup>I-MIBG scans and posttherapeutic <sup>131</sup>I-MIBG scans. <sup>123</sup>I-MIBG scans could detect lesions in 56% (64/115) of bone metastases, 64% (9/14) of lung metastases, 88% (15/17) of liver metastases, 75% (18/24) of metastases in others, and 62% (106/170) of all lesions compared with posttherapeutic <sup>131</sup>I-MIBG scans.

Figure 1 shows time-course changes of uptake ratios in 10 patients whose <sup>131</sup>I-MIBG scans were obtained at 3 days after <sup>131</sup>I-MIBG therapeutics. The uptake ratios were higher at a later scanning time. There were significant differences in the uptake ratios between 6 and 24 h of <sup>123</sup>I-MIBG (*P* = 0.031), 6 h of <sup>123</sup>I-MIBG and 3 days of <sup>131</sup>I-MIBG (*P* = 0.020), and 24 h of <sup>123</sup>I-MIBG and 3 days of <sup>131</sup>I-MIBG (*P* = 0.018).

Figures 2 and 3 show the representative scans of <sup>123</sup>I-MIBG and <sup>131</sup>I-MIBG. In Fig. 2, the 24-h image of <sup>123</sup>I-MIBG excelled in the lesion detectability compared with the 6-h image of <sup>123</sup>I-MIBG. The number of lesions between <sup>123</sup>I-MIBG and <sup>131</sup>I-MIBG was the same. However, the lesion was better visualized in the <sup>131</sup>I-MIBG image than in the <sup>123</sup>I-MIBG image, which was confirmed by the quantitative analysis using uptake ratios. Figure 3 shows that <sup>131</sup>I-MIBG was superior to <sup>123</sup>I-MIBG in both visual and quantitative assessment.

**Discussion**

In this study, we demonstrated with visual and quantitative methods that low-dose <sup>123</sup>I-MIBG (111 MBq)

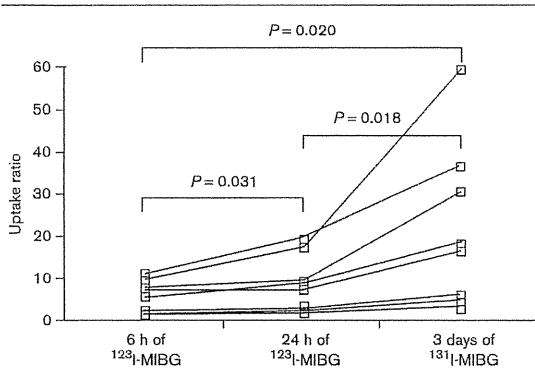
scans were not suitable for detecting lesions compared with posttreatment  $^{131}\text{I}$ -MIBG scans.

Our results were likely due to at least two reasons. First, the diagnostic dose of  $^{123}\text{I}$ -MIBG was significantly lower compared with the therapeutic dose of  $^{131}\text{I}$ -MIBG. In the report by Ali *et al.* [22], the combination of the modern

$\gamma$  camera with a low-energy collimator and  $^{123}\text{I}$  imaging showed a count rate of up to 20-fold greater compared with an equivalent activity of  $^{131}\text{I}$ , because of the characteristics of  $^{123}\text{I}$  and  $^{131}\text{I}$ . Therefore, a dose of 185 MBq of  $^{123}\text{I}$  was equivalent to almost 3.7 GBq of  $^{131}\text{I}$  in image quality in patients with thyroid cancer. Iwano *et al.* [23] reported that the diagnostic scan with 37 MBq of  $^{123}\text{I}$  was not always predictive of subsequent therapeutic  $^{131}\text{I}$  uptake in detecting residual thyroid tissue and metastases of differentiated thyroid cancer. Donahue *et al.* [24] concluded that posttreatment  $^{131}\text{I}$  whole-body scans provided incremental clinically relevant information in addition to pretreatment  $^{123}\text{I}$  whole-body scans in 10% of patients with differentiated thyroid cancer. Considering the same pharmaceutical kinetics of  $^{123}\text{I}$ -MIBG and  $^{131}\text{I}$ -MIBG, a diagnostic dose of  $^{123}\text{I}$ -MIBG was assumed to be equal in imaging quality to a 20-fold greater  $^{131}\text{I}$ -MIBG dose. In our study, the doses of  $^{123}\text{I}$ -MIBG (111 MBq) were less than one-fiftieth of the doses of  $^{131}\text{I}$ -MIBG (5.55–7.4 GBq). To improve the lesion detectability with  $^{123}\text{I}$ -MIBG, the dose of  $^{123}\text{I}$ -MIBG should be increased. Considering that the standard doses of  $^{131}\text{I}$ -MIBG therapy for malignant pheochromocytoma and paraganglioma are more than 7.4 GBq [25–27], more than 370 MBq of  $^{123}\text{I}$ -MIBG might be desirable to detect lesions of malignant pheochromocytoma and paraganglioma.

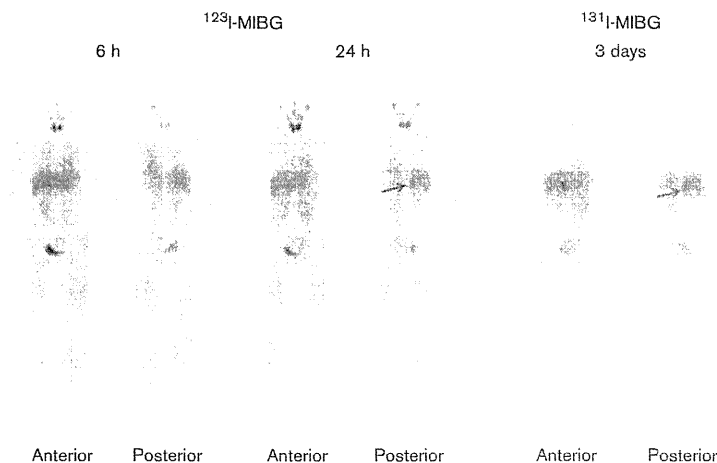
Another likely reason for our results was the difference of scanning time after MIBG injections between  $^{123}\text{I}$ -MIBG and  $^{131}\text{I}$ -MIBG. In this study, the 24-h images of  $^{123}\text{I}$ -MIBG could detect more lesions than the 6-h images of

Fig. 1



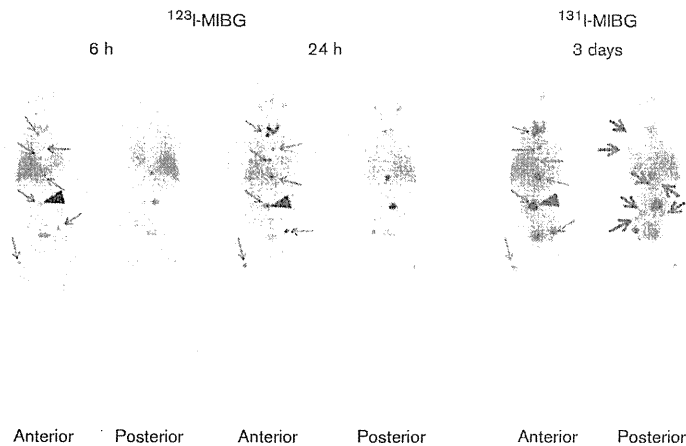
Time-course changes of uptake ratios. The uptake ratios are higher at later scanning time. As no abnormal accumulation is detected on the 6-h image of  $^{123}\text{I}$ -metaiodobenzylguanidine (MIBG) in patient number 12 in Tables 1 and 2, the paired *t*-tests are performed among nine patients between 6 and 24 h of  $^{123}\text{I}$ -MIBG and between 6 h of  $^{123}\text{I}$ -MIBG and 3 days of  $^{131}\text{I}$ -MIBG and among 10 patients between 24 h of  $^{123}\text{I}$ -MIBG and 3 days of  $^{131}\text{I}$ -MIBG.

Fig. 2



A 37-year-old woman with pheochromocytoma, patient number 12 in Tables 1 and 2. No abnormal accumulation is seen on the 6 h image of  $^{123}\text{I}$ -metaiodobenzylguanidine (MIBG). The 24-h image of  $^{123}\text{I}$ -MIBG can identify a faint accumulation in the right mid abdomen and the 3-day image of  $^{131}\text{I}$ -MIBG can identify a strong accumulation in the same lesion (arrows). No additional uptake is detected on the 3-day image of  $^{131}\text{I}$ -MIBG. Uptake ratios of the right mid abdomen lesion are 3.55 and 5.80 on the 24-h image of  $^{123}\text{I}$ -MIBG and the 3-day image of  $^{131}\text{I}$ -MIBG. The uptake ratio of the 6-h image of  $^{123}\text{I}$ -MIBG cannot be calculated because no lesional uptake is detected on the 6-h image of  $^{123}\text{I}$ -MIBG.

Fig. 3



A 78-year-old woman with pheochromocytoma, patient number 3 in Tables 1 and 2. A total of seven lesions are detected in the bone with the 6 and 24-h images of  $^{123}\text{I}$ -metaiodobenzylguanidine (MIBG, narrow arrows on each anterior image of  $^{123}\text{I}$ -MIBG). Same lesions are detected (narrow arrows on the anterior image of  $^{131}\text{I}$ -MIBG) and seven new lesions can be identified with the 3-day image of  $^{131}\text{I}$ -MIBG (wide arrows on the posterior image of  $^{131}\text{I}$ -MIBG). The uptake ratios of the lumbar spine (arrow heads on each anterior image of  $^{123}\text{I}$ -MIBG and  $^{131}\text{I}$ -MIBG) are 5.33, 9.21, and 27.07 on each image.

$^{123}\text{I}$ -MIBG in eight (53%) of 15 patients. Furthermore, the 2–5-day images of  $^{131}\text{I}$ -MIBG were superior to the 24-h images of  $^{123}\text{I}$ -MIBG in eight (53%) of 15 patients. As shown in Fig. 1, we demonstrated that the lesion-to-referent count ratios increased at later scanning time. These results indicated that early scan timing after  $^{123}\text{I}$ -MIBG injection was not recommended. The European Association of Nuclear Medicine guidelines suggest that scanning with  $^{123}\text{I}$ -MIBG is performed between 20 and 24 h after injection and selected delayed images (never later than day 2) might be useful in the event of equivocal findings on day 1 [13,28]. In contrast, the Japanese Ministry of Health, Labor and Welfare established that  $^{123}\text{I}$ -MIBG scanning was performed at 24 h after injection, and additional images might be obtained at 6 or 48 h after administration if needed. Our results indicated that 6-h images after  $^{123}\text{I}$ -MIBG injection would not be necessary. Even if small lesions or low-uptake lesions are located in or near the kidneys and excretory route that may be masked by uptake in these areas, 6-h images may not aid the visualization of lesions because physiological uptake of MIBG is more intense in early images than in late images.

Diagnostic scintigraphy with low-dose  $^{123}\text{I}$ -MIBG has limitations in detecting lesions of malignant pheochromocytoma and malignant paraganglioma. The possible discrepancy between low-dose diagnostic  $^{123}\text{I}$ -MIBG and posttreatment  $^{131}\text{I}$ -MIBG scans should be taken into account when developing a treatment plan. An  $^{131}\text{I}$ -MIBG posttreatment scan might provide us with more clinical information in patients with malignant pheochromocytoma and malignant paraganglioma. We recommended that patients who had

small lesions that were not detected with a low-dose  $^{123}\text{I}$ -MIBG scan but confirmed with other imaging modalities, such as CT and magnetic resonance imaging, be considered for  $^{131}\text{I}$ -MIBG therapy if their primary lesion that had been surgically excised had accumulated MIBG.

Our study had some limitations. One limitation was that the dose of  $^{123}\text{I}$ -MIBG of our study was lower than that of the standard dose of  $^{123}\text{I}$ -MIBG in Western countries. Another limitation was that the scanning speed of  $^{123}\text{I}$ -MIBG scintigraphy was higher than that recommended by European Association of Nuclear Medicine guidelines (15 cm/min compared with the guidance of 5 cm/min) [13]. The low-dose and the fast scanning speed of  $^{123}\text{I}$ -MIBG would decrease the signal-to-noise ratio compared with the high-dose and the slow scanning speed. Those would result in the reduction of not only the lesional detectability of visual evaluation but also the uptake ratio of quantitative evaluation of  $^{123}\text{I}$ -MIBG scintigraphy. In this study, we did not evaluate the detectability of single photon emission computed tomography/CT. This is now becoming popular as a daily practice. This would certainly enhance the detection of the lesion with in the areas of physiological uptake (e.g. liver) and the lesion that overlapped on the physiological uptake (e.g. bladder) on planar whole-body imaging.

### Conclusion

In conclusion, a low-dose diagnostic  $^{123}\text{I}$ -MIBG scan has limitations compared with posttreatment  $^{131}\text{I}$ -MIBG scan. Compared with a 24-h image of  $^{123}\text{I}$ -MIBG, a 6-h image of  $^{123}\text{I}$ -MIBG has no advantage in detecting lesions

of malignant pheochromocytoma and malignant paraganglioma. The escalation of  $^{123}\text{I}$ -MIBG doses might be beneficial for the diagnosis of distribution of metastasis.

### Acknowledgements

This research did not receive any support in the form of grants, equipment, drugs, or combination of these.

This research did not receive any funding from any of the following organizations: National Institutes of Health, Wellcome Trust, Howard Hughes Medical Institute, and others.

### Conflicts of interest

There are no conflicts of interest.

### References

- 1 Jaques S Jr., Tobes MC, Sisson JC. Sodium dependency of uptake of norepinephrine and m-iodobenzylguanidine into cultured human pheochromocytoma cells: evidence for uptake-one. *Cancer Res* 1987; **47**:3920–3928.
- 2 Ilias I, Pacak K. Current approaches and recommended algorithm for the diagnostic localization of pheochromocytoma. *J Clin Endocrinol Metab* 2004; **89**:479–491.
- 3 Wieland DM, Wu J, Brown LE, Mangner TJ, Swanson DP, Beierwaltes WH. Radiolabeled adrenergic neuron-blocking agents: adrenomedullary imaging with [ $^{131}\text{I}$ ]iodobenzylguanidine. *J Nucl Med* 1980; **21**:349–353.
- 4 Nakajo M, Shapiro B, Copp J, Kalf V, Gross MD, Sisson JC, et al. The normal and abnormal distribution of the adrenomedullary imaging agent m-[ $^{131}\text{I}$ ]iodobenzylguanidine (I-131 MIBG) in man: evaluation by scintigraphy. *J Nucl Med* 1983; **24**:672–682.
- 5 Sisson JC, Frager MS, Valk TW, Gross MD, Swanson DP, Wieland DM, et al. Scintigraphic localization of pheochromocytoma. *N Engl J Med* 1981; **305**:12–17.
- 6 Shapiro B, Copp JE, Sisson JC, Eyre PL, Wallis J, Beierwaltes WH. Iodine-131 metaiodobenzylguanidine for the locating of suspected pheochromocytoma: experience in 400 cases. *J Nucl Med* 1985; **26**:576–585.
- 7 Sisson JC, Shulkin BL. Nuclear medicine imaging of pheochromocytoma and neuroblastoma. *Q J Nucl Med* 1999; **43**:217–223.
- 8 Rufini V, Castaldi P, Treglia G, Perotti G, Gross MD, Al-Nahhas A, et al. Nuclear medicine procedures in the diagnosis and therapy of medullary thyroid carcinoma. *Biomol Pharmacother* 2008; **62**:139–146.
- 9 Jacobson AF, Deng H, Lombard J, Lessig HJ, Black RR.  $^{123}\text{I}$ -metaiodobenzylguanidine scintigraphy for the detection of neuroblastoma and pheochromocytoma: results of a meta-analysis. *J Clin Endocrinol Metab* 2010; **95**:2596–2606.
- 10 Furuta N, Kiyota H, Yoshigoe F, Hasegawa N, Ohishi Y. Diagnosis of pheochromocytoma using [ $^{123}\text{I}$ ] compared with [ $^{131}\text{I}$ ] metaiodobenzylguanidine scintigraphy. *Int J Urol* 1999; **6**:119–124.
- 11 Koopmans KP, Neels ON, Kema IP, Elsinga PH, Links TP, de Vries EG, et al. Molecular imaging in neuroendocrine tumors: molecular uptake mechanisms and clinical results. *Crit Rev Oncol Hematol* 2009; **71**:199–213.
- 12 Adler JT, Meyer-Rochow GY, Chen H, Benn DE, Robinson BG, Sippel RS, et al. Pheochromocytoma: current approaches and future directions. *Oncologist* 2008; **13**:779–793.
- 13 Bombardieri E, Giammarile F, Aktolun C, Baum RP, Bischof Delaloye A, Maffioli L, et al.  $^{131}\text{I}$ /123I-metaiodobenzylguanidine (mIBG) scintigraphy: procedure guidelines for tumour imaging. *Eur J Nucl Med Mol Imaging* 2010; **37**:2436–2446.
- 14 Taggart DR, Han MM, Quach A, Groshen S, Ye W, Villablanca JG, et al. Comparison of iodine-123 metaiodobenzylguanidine (MIBG) scan and [ $^{18}\text{F}$ ]fluorodeoxyglucose positron emission tomography to evaluate response after iodine-131 MIBG therapy for relapsed neuroblastoma. *J Clin Oncol* 2009; **27**:5343–5349.
- 15 Sharp SE, Shulkin BL, Gelfand MJ, Salisbury S, Furman WL.  $^{123}\text{I}$ -MIBG scintigraphy and  $^{18}\text{F}$ -FDG PET in neuroblastoma. *J Nucl Med* 2009; **50**:1237–1243.
- 16 Papatheanasiou ND, Gaze MN, Sullivan K, Aldridge M, Waddington W, Almuhaideb A, et al.  $^{18}\text{F}$ -FDG PET/CT and  $^{123}\text{I}$ -metaiodobenzylguanidine imaging in high-risk neuroblastoma: diagnostic comparison and survival analysis. *J Nucl Med* 2011; **52**:519–525.
- 17 Timmers HJ, Chen CC, Carrasquillo JA, Whatley M, Ling A, Havekes B, et al. Comparison of  $^{18}\text{F}$ -fluoro-L-DOPA,  $^{18}\text{F}$ -fluoro-deoxyglucose, and  $^{18}\text{F}$ -fluorodopamine PET and  $^{123}\text{I}$ -MIBG scintigraphy in the localization of pheochromocytoma and paraganglioma. *J Clin Endocrinol Metab* 2009; **94**:4757–4767.
- 18 Kroiss A, Putzer D, Uppimny C, Decristoforo C, Gabriel M, Santner W, et al. Functional imaging in pheochromocytoma and neuroblastoma with  $^{68}\text{Ga}$ -DOTA-Tyr 3-octetotide positron emission tomography and  $^{123}\text{I}$ -metaiodobenzylguanidine. *Eur J Nucl Med Mol Imaging* 2011; **38**:865–873.
- 19 Campbell L, Mouratidis B, Sullivan P. Improved detection of disseminated pheochromocytoma using post therapy I-131 MIBG scanning. *Clin Nucl Med* 1996; **21**:960–963.
- 20 Fukuoka M, Taki J, Mochizuki T, Kiruya S. Comparison of diagnostic value of I-123 MIBG and high-dose I-131 MIBG scintigraphy including incremental value of SPECT/CT over planar image in patients with malignant pheochromocytoma/paraganglioma and neuroblastoma. *Clin Nucl Med* 2011; **36**:1–7.
- 21 Rufini V, Calcagni ML, Baum RP. Imaging of neuroendocrine tumors. *Semin Nucl Med* 2006; **36**:228–247.
- 22 Ali N, Sebastian C, Foley RR, Murray I, Canizales AL, Jenkins PJ, et al. The management of differentiated thyroid cancer using  $^{123}\text{I}$  for imaging to assess the need for  $^{131}\text{I}$  therapy. *Nucl Med Commun* 2006; **27**:165–169.
- 23 Iwano S, Kato K, Nishashi T, Ito S, Tachi Y, Naganawa S. Comparisons of I-123 diagnostic and I-131 post-treatment scans for detecting residual thyroid tissue and metastases of differentiated thyroid cancer. *Ann Nucl Med* 2009; **23**:777–782.
- 24 Donahue KP, Shah NP, Lee SL, Oates ME. Initial staging of differentiated thyroid carcinoma: continued utility of posttherapy  $^{131}\text{I}$  whole-body scintigraphy. *Radiology* 2008; **246**:887–894.
- 25 Gedik GK, Hoefnagel CA, Bais E, Olmos RA.  $^{131}\text{I}$ -MIBG therapy in metastatic pheochromocytoma and paraganglioma. *Eur J Nucl Med Mol Imaging* 2008; **35**:725–733.
- 26 Safford SD, Coleman RE, Gockerman JP, Moore J, Feldman JM, Leight GS Jr., et al. Iodine-131 metaiodobenzylguanidine is an effective treatment for malignant pheochromocytoma and paraganglioma. *Surgery* 2003; **134**:956–962; discussion 962–963.
- 27 Fitzgerald PA, Goldsby RE, Huberty JP, Price DC, Hawkins RA, Veatch JJ, et al. Malignant pheochromocytomas and paragangliomas: a phase II study of therapy with high-dose  $^{131}\text{I}$ -metaiodobenzylguanidine ( $^{131}\text{I}$ -MIBG). *Ann N Y Acad Sci* 2006; **1073**:465–490.
- 28 Olivier P, Colarinha P, Feticch J, Fischer S, Frokier J, Giammarile F, et al. Guidelines for radioiodinated MIBG scintigraphy in children. *Eur J Nucl Med Mol Imaging* 2003; **30**:B45–B50.

# Comparison of Diagnostic Value of I-123 MIBG and High-Dose I-131 MIBG Scintigraphy Including Incremental Value of SPECT/CT Over Planar Image in Patients With Malignant Pheochromocytoma/Paraganglioma and Neuroblastoma

Makoto Fukuoka, MD,\* Junichi Taki, MD, PhD,\* Takafumi Mochizuki, MD, PhD,\*  
and Seigo Kinuya, MD, PhD†

**Purpose:** To compare lesion detectability of I-123 MIBG scintigraphy with that of high-dose I-131 MIBG and to evaluate incremental benefit of SPECT/CT over planar image for the detection and localization of the lesions in patients with I-131 MIBG therapy for malignant pheochromocytoma/paraganglioma and neuroblastoma.

**Materials and Methods:** We retrospectively investigated 16 patients with malignant pheochromocytoma/paraganglioma and neuroblastoma, who were referred for I-131 MIBG therapy. We investigated the lesion detectability in 10 pairs of I-123 and high-dose I-131 MIBG studies of the same patient, obtained within 2 weeks. In 31 studies of I-123 MIBG scintigraphy in 16 patients and 17 studies of high-dose I-131 MIBG scintigraphy in 12 patients, we compared planar and SPECT/CT images for the lesion detectability and localization.

**Results:** The number of lesions detected by I-123 MIBG planar image and SPECT/CT and high-dose planar I-131 MIBG and SPECT/CT were 3.0 and 3.7, 7.3 and 7.7 per study, respectively. SPECT/CT images provided additional diagnostic information over planar images in 25 studies (81%) of 12 patients (75%) in I-123 MIBG scintigraphy and in 9 studies (53%) of 9 patients (75%) in high-dose I-131 MIBG scintigraphy.

**Conclusion:** Post-therapy high-dose I-131 MIBG scintigraphy is superior to I-123 MIBG scintigraphy in lesion detectability even in comparison with I-123 MIBG SPECT/CT images and high-dose I-131 MIBG planar images in patients with malignant neuroendocrine tumors. SPECT/CT images are helpful for accurate identification of anatomic localization compared with planar images.

**Key Words:** malignant neuroendocrine tumor, I-123-MIB, I-131 MIBG, SPECT/CT

(*Clin Nucl Med* 2011;36: 1–7)

Metaiodobenzylguanidine (MIBG) is a guanethidine derivative resembling the neurotransmitter norepinephrine in chemical structure. Therefore, showing the similar performance as norepinephrine, MIBG is taken up by the norepinephrine transporter (uptake 1) or passive diffusion, and stored in chromaffin deposit granules or neurosecretory granules in tissues derived from sympathetic nervous system.<sup>1,2</sup> In this mechanism, MIBG accumulates in tumors originated from neural crests.

Received for publication March 26, 2010; accepted July 6, 2010.

From the \*Department of Nuclear Medicine, Kanazawa University Hospital, Kanazawa, Japan; and †Department of Biotracer Medicine, Kanazawa University Graduate School of Medical Sciences, Kanazawa, Japan.

There are no financial disclosures from any authors.

Reprints: Junichi Taki, MD, PhD, Department of Nuclear Medicine, Kanazawa University Hospital, 13-1 Takara-machi, Kanazawa, 920-8640, Japan. E-mail: taki@med.kanazawa-u.ac.jp.

Copyright © 2010 by Lippincott Williams & Wilkins

ISSN: 0363-9762/11/3601-0001

Pheochromocytoma/paraganglioma and neuroblastoma are the representative neuroendocrine neoplasms showing intense MIBG accumulation. Pheochromocytoma/paraganglioma is a rare tumor which arises from chromaffin cells of the adrenal medulla/extra-adrenal sympathetic ganglia. It is reported that approximately 10% of pheochromocytoma and up to 40% of paraganglioma are malignant.<sup>3,4</sup> Neuroblastoma is one of the most common tumor derived from the embryonal sympathetic nervous system in children. Approximately 30% of neuroblastoma originate from the adrenal medulla and the rest arise from anywhere extra-adrenal sympathetic nervous system.<sup>5,6</sup> Malignant pheochromocytoma/paraganglioma and neuroblastoma usually metastasize to the bones, liver, lung, and lymph nodes in early times.

Since I-131 labeled MIBG scintigraphy for pheochromocytoma was reported in 1981, I-131 and I-123 labeled MIBG scintigraphy has been widely used as an excellent functional imaging modality for detection of the lesions in patients with neuroendocrine tumors.<sup>7–9</sup> MIBG scintigraphy is also useful for detection of the recurrent or metastatic lesions in patients with malignant pheochromocytoma/paraganglioma and neuroblastoma, although it is reported that the sensitivity in detecting extra-adrenal or malignant tumors is less than that in adrenal or benign tumors.<sup>10–13</sup> In the image quality and lesion detectability, I-123 MIBG image is superior to I-131 MIBG with diagnostic low radioactive dose,<sup>14,15</sup> because the  $\gamma$ -ray energy of I-123 (159 keV) is more suitable for scintigraphy compared with that of I-131 (364 keV). In addition to low-dose I-123 MIBG imaging, high-dose I-131 MIBG imaging is possible in patients who underwent I-131 MIBG internal radiation therapy, which is a precious option of the systemic treatments especially in those patients who have irresectable or multiple metastatic lesions. A case report demonstrated that post-therapeutic high-dose I-131 MIBG scintigraphy detected more lesions than low-dose diagnostic I-123 MIBG scintigraphy in a patient underwent I-131 MIBG therapy.<sup>16</sup> Similar findings were observed in the diagnostic I-123 and high-dose post-treatment I-131 scintigraphy in thyroid cancer.<sup>17</sup>

Accurate identification of anatomic localization of the lesions is important to perform I-131 MIBG therapy safely. However, it is difficult to identify accurate anatomic localization of the lesions in the conventional planar image. Comparing SPECT with CT or MRI image side-by-side or SPECT-CT or MRI fusion image by use of software has contributed to the precise definition of the localization to some degree.<sup>18–20</sup> Recently, integrated SPECT/CT fusion system which acquires the dual modality in the same session provides more additional information for characterization and localization of the lesions in various neuroendocrine tumors.<sup>21–26</sup>

The aim of this study was to compare lesion detectability of the I-123 MIBG scintigraphy with that of high-dose I-131 MIBG scintigraphy and to evaluate incremental benefit of I-123 MIBG and high-dose I-131 MIBG SPECT/CT over conventional planar image



TABLE 1. Clinical Characteristics of Patients

| Patient Number | Age | Sex | Diagnosis | No. I-131 MIBG Therapy | Cumulative Dose of I-131MIBG (mCi) | No. I-123 MIBG Scintigraphy | No. High-Dose I-131 MIBG Scintigraphy |
|----------------|-----|-----|-----------|------------------------|------------------------------------|-----------------------------|---------------------------------------|
| 1              | 69  | M   | pheo      | 2                      | 400                                | 3                           | 2                                     |
| 2              | 37  | F   | phico     | 2                      | 400                                | 3                           | 2                                     |
| 3              | 60  | F   | pheo      | 2                      | 400                                | 3                           | 2                                     |
| 4              | 63  | M   | para      | 1                      | 200                                | 3                           | 1                                     |
| 5              | 66  | M   | pheo      | 3                      | 600                                | 2                           | 0                                     |
| 6              | 54  | F   | para      | 1                      | 200                                | 3                           | 1                                     |
| 7              | 47  | M   | pheo      | 4                      | 1360                               | 2                           | 1                                     |
| 8              | 36  | M   | para      | 0                      | 0                                  | 1                           | 0                                     |
| 9              | 7   | F   | neuro     | 1                      | 100                                | 1                           | 1                                     |
| 10             | 8   | M   | neuro     | 0                      | 0                                  | 1                           | 0                                     |
| 11             | 13  | F   | neuro     | 3                      | 600                                | 3                           | 3                                     |
| 12             | 7   | M   | neuro     | 1                      | 300                                | 1                           | 1                                     |
| 13             | 11  | F   | neuro     | 1                      | 400                                | 1                           | 1                                     |
| 14             | 7   | F   | neuro     | 1                      | 300                                | 1                           | 1                                     |
| 15             | 8   | F   | neuro     | 1                      | 100                                | 2                           | 0                                     |
| 16             | 10  | M   | neuro     | 1                      | 400                                | 1                           | 1                                     |

MIBG indicates metaiodobenzylguanidine; pheo, malignant pheochromocytoma; para, malignant paraganglioma; neuro, neuroblastoma.

TABLE 2. The Number of Detected Lesions in 10 Pairs of I-123 and High-Dose I-131 MIBG Scintigraphies Performed Within 2 Weeks in the Same Patient

| Patient Number | I-123 MIBG   |                     | I-131 MIBG Planar Image | I-131 MIBG SPECT/CT |
|----------------|--------------|---------------------|-------------------------|---------------------|
|                | Planar Image | I-123 MIBG SPECT/CT |                         |                     |
| 1              | 0            | 1                   | 1                       | 1                   |
| 2              | 6            | 6                   | 6                       | 6                   |
| 3              | 1            | 2                   | 4                       | 6                   |
| 4              | 1            | 1                   | 1                       | 1                   |
| 5              | 1            | 3                   | 15                      | 15                  |
| 6              | 1            | 2                   | 8                       | 9                   |
| 7              | 2            | 2                   | 7                       | 7                   |
| 8              | 0            | 0                   | 3                       | 2                   |
| 9              | 15           | 15                  | 15                      | 17                  |
| 10             | 3            | 5                   | 13                      | 13                  |
| Total          | 30           | 37                  | 73                      | 77                  |

MIBG indicates metaiodobenzylguanidine.

for the detection and localization of the lesions in patients who underwent I-131 MIBG therapy for malignant pheochromocytoma/paraganglioma and neuroblastoma.

## MATERIALS AND METHODS

### Patients

We retrospectively investigated 16 patients with malignant pheochromocytoma/paraganglioma and neuroblastoma, who were referred for I-131 MIBG therapy in our institute and underwent I-123 MIBG (111 MBq [3 mCi]) and/or high-dose I-131 MIBG (3.7–14.8 GBq [100–400 mCi]) scintigraphy from June 2008 to August 2009 (5 males and 3 females with malignant pheochromocytoma/paraganglioma, mean age 54 years [range, 36–69 years]; 3 males and 5 females with neuroblastoma, mean age 8.8 years [range, 7–13 years] (Table 1). Thirty-one studies of I-123 MIBG scintigra-

phy were obtained in 16 patients and 17 studies of high-dose I-131 MIBG scintigraphy were acquired in 12 patients.

### I-123 MIBG Scintigraphy With Diagnostic Low-Radioactive Dose

I-123 MIBG scintigraphy was performed after intravenous injection of 111 MBq (3 mCi) of radiopharmaceutical for all patients, using a dual-head gamma camera equipped with a low-intermediate energy collimator and a 5/8 inch NaI crystal, which was combined to a low-dose spiral CT by the same gantry (Symbia, Siemens Medical Solutions). Whole-body planar images were acquired at 6 and 24 hours after I-123 MIBG injection at scanning speeds of 15 cm/min. Following planar imaging after 6 hours of tracer injection, SPECT images were obtained to cover the areas suspected of abnormal tracer accumulations in whole-body planar images. SPECT data were acquired from 60 projections (20 seconds per view) with 128 × 128 matrix and reconstructed using a 3-dimensional iterative algorithm, ordered-subsets expectation maximization. As soon as SPECT data acquisition was finished, CT transmission scans for tomography were performed. SPECT and CT data were analyzed and coregistered using an e-soft workstation.

### I-131 MIBG Therapy and Scintigraphy With Post-Therapy High-Radioactive Dose

I-131 MIBG therapy was administered to the patients who were considered to have beneficial therapeutic effects through the findings of pretherapy I-123 MIBG scintigraphy. 3.7–14.8 GBq (100–400 mCi) of I-131 MIBG was injected intravenously through fixed peripheral venous lines for about an hour, using lead-shielded infusion pump. Vital signs were monitored for more than 6 hours from the beginning of I-131 MIBG administration. I-131 MIBG planar and SPECT/CT images were acquired 3 days later in the same way as I-123 MIBG scintigraphy, except for the use of collimator (high-energy).

### Image Interpretation

At first, I-123 or I-131 MIBG planar images were evaluated by 2 experienced nuclear medicine physicians, who were blinded to the findings of the other imaging modalities. They were asked to interpret all focal uptakes, except for physiological accumulation, as

**TABLE 3.** Number of Lesions in I-123 MIBG Imaging

| Study Number | Diagnosis | No. Lesions in Planar Image | No. Lesions in SPECT/CT | No. Newly Detected Lesions in SPECT/CT | No. Lesions Turned to be Negative in SPECT/CT | No. Lesions Modified Anatomical Localization by SPECT/CT |
|--------------|-----------|-----------------------------|-------------------------|--|---|--|
| 1            | neuro     | 0                           | 0                       | 0                                      | 0   | 0  |
| 2            | para      | 1                           | 2                       | 1                                      | 0   | 1  |
| 3            | pheo      | 2                           | 3                       | 1                                      | 0   | 0  |
| 4            | neuro     | 2                           | 3                       | 1                                      | 0   | 1  |
| 5            | pheo      | 1                           | 1                       | 0                                      | 0   | 0  |
| 6            | pheo      | 6                           | 6                       | 0                                      | 0   | 2  |
| 7            | pheo      | 3                           | 4                       | 1                                      | 0   | 0  |
| 8            | pheo      | 0                           | 1                       | 1                                      | 0   | 0  |
| 9            | neuro     | 1                           | 1                       | 0                                      | 0   | 0  |
| 10           | para      | 2                           | 3                       | 1                                      | 0   | 1  |
| 11           | para      | 25                          | 25                      | 0                                      | 0   | 2  |
| 12           | neuro     | 3                           | 5                       | 2                                      | 0   | 0  |
| 13           | neuro     | 0                           | 0                       | 0                                      | 0   | 0  |
| 14           | neuro     | 23                          | 18                      | 0                                      | 5   | 3  |
| 15           | neuro     | 1                           | 2                       | 1                                      | 0   | 1  |
| 16           | neuro     | 1                           | 3                       | 2                                      | 0   | 0  |
| 17           | para      | 1                           | 2                       | 1                                      | 0   | 1  |
| 18           | pheo      | 2                           | 2                       | 0                                      | 0   | 1  |
| 19           | neuro     | 1                           | 1                       | 0                                      | 0   | 0  |
| 20           | pheo      | 2                           | 2                       | 0                                      | 0   | 0  |
| 21           | pheo      | 1                           | 3                       | 2                                      | 0   | 0  |
| 22           | pheo      | 3                           | 3                       | 0                                      | 0   | 0  |
| 23           | pheo      | 1                           | 1                       | 0                                      | 0   | 1  |
| 24           | para      | 16                          | 16                      | 0                                      | 0   | 2  |
| 25           | neuro     | 2                           | 2                       | 1                                      | 1   | 0  |
| 26           | pheo      | 3                           | 4                       | 1                                      | 0   | 0  |
| 27           | pheo      | 1                           | 1                       | 0                                      | 0   | 0  |
| 28           | pheo      | 3                           | 3                       | 0                                      | 0   | 1  |
| 29           | pheo      | 1                           | 1                       | 1                                      | 1   | 0  |
| 30           | para      | 22                          | 22                      | 0                                      | 0   | 3  |
| 31           | neuro     | 15                          | 15                      | 1                                      | 1   | 1  |
| Total        |           | 145                         | 155                     | 18                                     | 8   | 21   |

MIBG indicates metaiodobenzylguanidine; pheo, malignant pheochromocytoma; para, malignant paraganglioma; neuro, neuroblastoma.

abnormal lesions and to define their anatomic locations. Diffuse accumulation at nasal cavity, salivary glands, thyroid, myocardium, liver, and bladder was considered as physiological uptake. When their interpretations were discordant, consensus was obtained after a conference. Then, SPECT/CT images were assessed by them independently with planar images and they were required to re-evaluate the anatomic location of the lesions found in planar images and indicate new lesions. The findings suspected of metastasis in CT images alone were not included in new lesions if they did not accompany MIBG accumulation. Consensus was acquired in the same way as planar image if their interpretation was discordant.

**Data Analysis**

In comparison of diagnostic value of I-123 MIBG and high-dose I-131 MIBG scintigraphy, we investigated the difference of the number of detected lesions in 10 pairs of I-123 and high-dose I-131 MIBG studies of the same patient that were obtained within 2 weeks. In the evaluation of incremental diagnostic value of SPECT/CT images over planar images with I-123 MIBG and high-dose I-131 MIBG, we performed comparative analysis between planar and SPECT/CT images in all patients.

**RESULTS**

In I-123 MIBG scintigraphy, a total of 145 and 155 abnormal uptakes were pointed out in planar and SPECT/CT images, respectively, in 31 studies of 16 patients. In high-dose I-131 MIBG scintigraphy, a total of 136 and 140 abnormal uptakes were pointed out in planar and SPECT/CT images, respectively, in 17 studies of 12 patients.

In comparison of all 10 pairs of I-123 and high-dose I-131 MIBG studies in the same patient that were obtained within 2 weeks, the lesions detected by I-123 MIBG scintigraphy were 3.0/study in planar image, 3.7/study in SPECT/CT image; and the lesions detected by high-dose I-131 MIBG scintigraphy were 7.3/study in planar image, 7.7/study in SPECT/CT images. The number of detected lesions is summarized in Table 2.

In all I-123 MIBG SPECT/CT images, 18 new lesions, which had not been pointed out in planar images, were detected in 14 studies (45.2%) of 11 patients (68.8%), but 8 lesions which had been recognized in planar images became undetectable in 4 studies (12.9%) of 2 patients (12.5%). Anatomic locations of 21 lesions in planar image were modified after analysis of SPECT/CT images in 14 studies (45.2%) of 10 patients (62.5%). As a whole, SPECT/CT

**TABLE 4.** Number of Lesions in High-Dose I-131 MIBG Imaging

| Study Number | Diagnosis | No. Lesions in Planar Image | No. Lesions in SPECT/CT | No. Newly Detected Lesions in SPECT/CT | No. Lesions Turned to be Negative in SPECT/CT | No. Lesions Modified Anatomical Localization by SPECT/CT |
|--------------|-----------|-----------------------------|-------------------------|--|---|--|
| 1            | pheo      | 2                           | 2                       | 0                                      | 0   | 0  |
| 2            | pheo      | 1                           | 1                       | 0                                      | 0   | 0  |
| 3            | pheo      | 6                           | 6                       | 0                                      | 0   | 0  |
| 4            | pheo      | 5                           | 6                       | 1                                      | 0   | 0  |
| 5            | para      | 4                           | 6                       | 2                                      | 0   | 3  |
| 6            | para      | 35                          | 35                      | 0                                      | 0   | 3  |
| 7            | pheo      | 2                           | 2                       | 0                                      | 0   | 0  |
| 8            | pheo      | 3                           | 3                       | 0                                      | 0   | 0  |
| 9            | pheo      | 7                           | 7                       | 0                                      | 0   | 1  |
| 10           | neuro     | 1                           | 1                       | 0                                      | 0   | 0  |
| 11           | neuro     | 15                          | 15                      | 0                                      | 0   | 1  |
| 12           | neuro     | 9                           | 8                       | 0                                      | 1   | 0  |
| 13           | neuro     | 8                           | 9                       | 1                                      | 0   | 2  |
| 14           | neuro     | 7                           | 7                       | 0                                      | 0   | 0  |
| 15           | neuro     | 3                           | 2                       | 0                                      | 1   | 1  |
| 16           | neuro     | 15                          | 17                      | 2                                      | 0   | 5  |
| 17           | neuro     | 13                          | 13                      | 0                                      | 0   | 1  |
| Total        |           | 136                         | 140                     | 6                                      | 2   | 17   |

MIBG indicates metaiodobenzylguanidine; pheo, malignant pheochromocytoma; para, malignant paraganglioma; neuro, neuroblastoma.

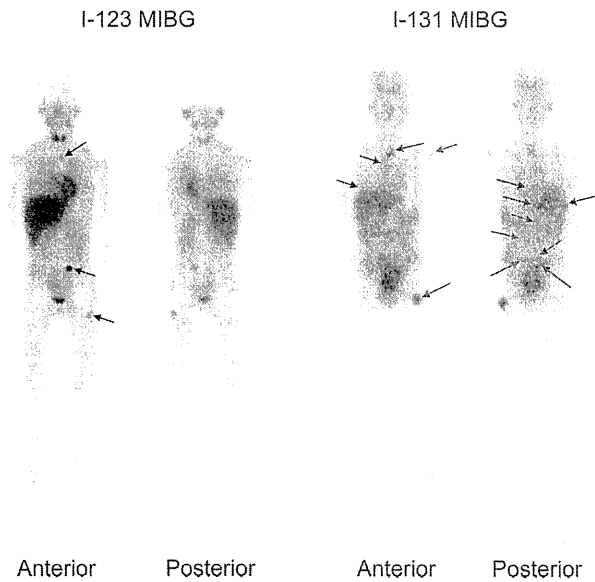


**FIGURE 1.** A 10-year-old boy with neuroblastoma underwent 14.8 GBq (400 mCi) of I-131 MIBG therapy. In the planar image with diagnostic I-123 MIBG, only 3 abnormal uptakes were detected in the upper mediastinum, left lower abdomen, and left thigh. In the planar image with therapeutic high-dose I-131 MIBG, total of 13 abnormal uptakes were detected in the left shoulder, mediastinum, vertebrae, upper and lower abdomen, and in the left thigh.

images provided additional diagnostic information over planar images in 25 studies (80.6%) of 12 patients (75.0%). The number of the lesions detected in I-123 MIBG planar and SPECT/CT imaging is summarized in Table 3.

In high-dose I-131 MIBG SPECT/CT images, 6 new lesions were detected in 4 studies (23.5%) of 4 patients (33.3%), but 2 lesions which had been recognized in planar images became obscure in 2 studies (11.8%) of 2 patients (16.7%). Anatomic locations of 17

lesions were altered after the evaluation of SPECT/CT images in 8 studies (47.1%) of 8 patients (66.7%). As a whole, SPECT/CT images provided additional diagnostic information in 9 studies (52.9%) of 9 patients (75.0%) over planar images. The number of the lesions in high-dose I-131 MIBG planar and SPECT/CT imaging is summarized in Table 4.

Most of the new lesions detected in SPECT/CT were located near the physiological uptake or were overlapped with the physio-

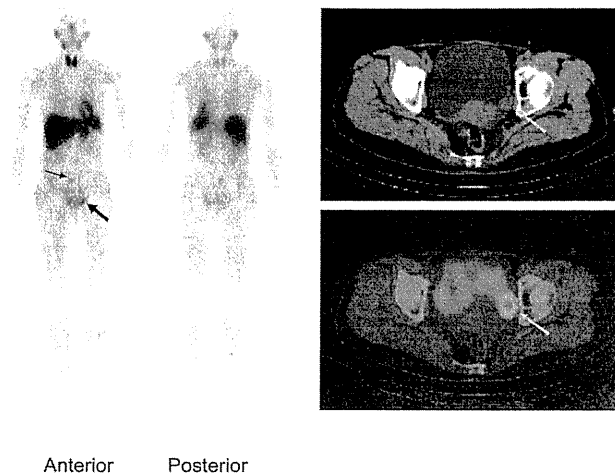


**FIGURE 2.** A 54-year-old woman with malignant paraganglioma underwent diagnostic I-123 MIBG scintigraphy. In the planar image, it is easy to point out the abnormal accumulation in the lower abdomen (narrow arrow), however, it is difficult to detect the abnormal uptake beside the bladder (wide arrow) because of physiological accumulation in the bladder. In the SPECT/CT, it is easy to detect the abnormal MIBG accumulation corresponding to the nodular lesion in the left side of the bladder.

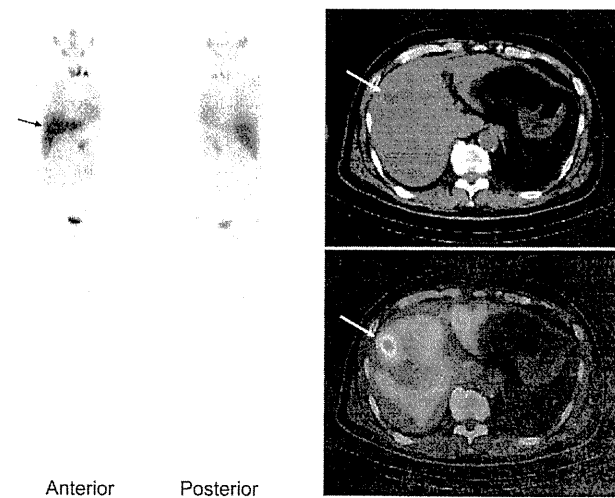


**FIGURE 3.** A 47-year-old woman with malignant pheochromocytoma underwent diagnostic low-dose I-123 MIBG scintigraphy. In the planar image, it is difficult to determine whether the abnormal uptake in the right upper abdomen exists in the right rib or in the liver. In the SPECT/CT, it is proved that the abnormal accumulation exists in the liver.

logical accumulation. In I-123 MIBG SPECT/CT images, 10 of 18 newly detected lesions by SPECT/CT were overlapped with the physiological accumulation and 1 new lesion was detected as a lymph node, 4 were in bones, and 3 were in lungs. In high-dose I-131 MIBG SPECT/CT images, 4 of 6 newly detected lesions were overlapped with the physiological accumulation and other one lesion was detected as a lymph node and another one was in a bone. All of the lesions turned to be negative in SPECT/CT were suspected to be located in bones in planar images.

The representative comparative planar images with I-123 MIBG and high-dose I-131 MIBG of a 10-year-old male patient with neuroblastoma are shown in Figure 1. A representative case with beneficial I-123 MIBG SPECT/CT over planar image for the detection of the lesion is shown in Figure 2. A case with beneficial

SPECT/CT over planar image for the localization of the abnormal uptake is shown in Figure 3.

#### DISCUSSION

I-131 MIBG internal radiation therapy has become popular as a systemic therapy for patients with malignant neuroendocrine tumors such as malignant pheochromocytoma, malignant paraganglioma, and neuroblastoma with metastatic lesions<sup>27-30</sup> in addition to chemotherapy represented by combined regimen of cyclophosphamide, vincristine, and dacarbazine.<sup>31</sup> For the indication of I-131 MIBG therapy, it is essential to confirm MIBG accumulation to the metastatic lesions and to rule out MIBG accumulation to high-risk sites such as the lesion compressing spinal cord. In our institute,